Magnetic couplings and exchange bias in Fe/NiO epitaxial layers

P. Luches,[1] S. Benedetti,[1] A. di Bona,[1] and S. Valeri[1,2]
[1]*Centro S3, CNR-Istituto di Nanoscienze, Via G. Campi 213/a, I-41125 Modena, Italy*
[2]*Dipartimento di Fisica, Università di Modena e Reggio Emilia, Via G. Campi 213/a, I-41125 Modena, Italy*
(Received 26 November 2009; revised manuscript received 28 January 2010; published 22 February 2010)

We report an investigation of the magnetic properties of Fe films epitaxially grown on NiO layers with (001) orientation. The results are interpreted with the help of a morphological characterization of the system. The onset of ferromagnetic behavior for the Fe layer is observed at 8 ML and it is ascribed to the coalescence of the islands, formed by Fe at the first stages of the growth, into larger interconnected islands. At larger Fe layer thickness the magnetization reversal is explained by taking into account the interplay between a unidirectional anisotropy, due to coupling with NiO, and the uniaxial growth anisotropy of Fe, which develops around 50 ML Fe layer thickness. No significant chemical modification of the interface is observed for thermal treatments up to 540 K. Exchange bias can be induced only for NiO layer thickness above 25 ML and its value can be tuned by changing the ferromagnetic to antiferromagnetic layer thickness ratio, reaching 220 Oe. No training effect is observed for this system.

DOI: 10.1103/PhysRevB.81.054431 PACS number(s): 75.70.Cn, 75.60.Jk, 75.60.Ej, 68.55.J−

I. INTRODUCTION

In order to explain and optimize a number of processes based on the magnetic properties of materials, such as for example tunneling magneto-resistance or exchange bias (EB), the use of epitaxial systems has shown to be very important.[1–3] In these systems it is possible to obtain an atomic-scale characterization of the structure and composition, and consequently, with the help of theoretical models, to achieve a good control of a large number of parameters. In particular, the role of the interface in many observed processes has been often recognized to be determinant for the overall behavior of the system.[3–6] Studies of epitaxial systems thoroughly characterized in the structure, morphology, and chemistry of the interfaces involved can be therefore of great help in understanding the properties of more complex materials.

In the case of the EB effect, i.e., the unidirectional anisotropy occurring at ferromagnetic (FM)/antiferromagnetic (AF) interfaces,[7–9] a general quantitative explanation is still not available. This is probably due to the complex atomic and magnetic configurations of real interfaces, which are difficult to be taken into account in the different models.[10–14]

NiO is an appealing AF material for the applications, because of its Néel temperature (520 K), significantly higher than room temperature (RT). The NiO(001) surface is a fully compensated AF surface; the spins are aligned along the ⟨112⟩ directions with 24 possible domains in the bulk.[15] When NiO is in the form of thin films the influence of the interface, of the surface and of the possible strain have been shown to preferentially stabilize some of the domains with respect to others.[15–17] In the case of thin NiO films on Ag(001), domains with the main spin component in the surface plane have been shown to be preferentially occupied.[16,17]

NiO has often been used as an AF material[15–17] for its simple rock-salt structure with a small lattice mismatch both with nonmagnetic materials such as Ag or MgO, used as substrates for its epitaxial growth,[18–21] and with 3*d* metals such as Fe and Co.[22–28] In particular, good quality epitaxial Fe layers have been obtained on NiO(001),[23,24,28] in spite of the occurrence of some NiO reduction and Fe oxidation at the interface.[22–25,28] In previous works we have performed a multitechnique characterization of the Fe/NiO interface, which allowed to obtain a detailed atomic scale model of its structure and composition.[24,25,28] These studies demonstrated that the oxidized Fe phase remains confined at the interface, where a FeO-like layer is formed,[25] while the metallic Ni, which results from the oxide-substrate reduction, is intermixed within the Fe film, forming an alloy with a distorted bcc structure involving ~3 ML.[28] The observed complex atomic structure at the interface is expected to have significant consequences on the magnetic behavior of Fe in this epitaxial FM/AF system.

In a 0.9 nm thick Fe film grown on bulk NiO(001) the Fe spin polarization was found to be in plane and almost perpendicular to the easy-spin axis of NiO,[29] in contrast with the case of other transition metals on NiO,[2,30,31] where a collinear coupling was observed. A micromagnetic simulation showed that for compensated FM/AF interfaces the equilibrium coupling is perpendicular, but a transition to parallel coupling is observed as the number of uncompensated moments at the interface is increased.[32] The values of EB field measured on similar systems, such as for example FM/NiO bilayers or polycrystalline Fe/NiO are a few tens of Oe at room temperature.[33,34]

In this study we investigate the magnetic properties of Fe epitaxial layers on NiO in a wide coverage range for both the AF and FM layers, and we show that the use of atomic-scale controlled systems allows achieving a good degree of control of the magnetic properties and of the dominant mechanisms which influence magnetization reversal. The good crystal quality allows obtaining larger values of EB at room temperature, compared to polycrystalline systems of the FM/NiO type, and no significant training effect.

II. EXPERIMENTAL

The samples were prepared in a ultrahigh vacuum (UHV) chamber by means of molecular beam epitaxy using a

Ag(001) single crystal as a substrate. The Ag surface was prepared by repeated cycles of sputtering and annealing. The NiO films were grown on the Ag substrate, kept at 460 K, by reactive evaporation of Ni from a Knudsen cell in an O_2 partial pressure of $\sim 1 \times 10^{-7}$ Torr. The Fe films were subsequently grown on the NiO layers at RT, using a Knudsen cell. Both Ni and Fe evaporation cells were oriented at 45° from sample normal, while the in plane orientation of the flux was oriented (by changing the in-plane orientation of the sample) to have the possible growth anisotropies (observed on similar systems in the direction perpendicular to the growth axis) as close as possible to the intrinsic anisotropy directions of the epitaxial films. This was done in order to simplify as much as possible the resulting magnetic system in terms of anisotropy directions. During NiO growth the in-plane orientation was at ~20° from Ag [010] direction, in order to align the expected growth anisotropy as close as possible to the NiO [121]. During Fe evaporation, the in-plane orientation of the Fe flux was along the NiO [110] direction, i.e., along the [100] direction of the growing Fe film, an easy magnetization direction in crystalline Fe films due to magnetocrystalline anisotropy. The metal flux rate was calibrated before the growth by a quartz microbalance. In the following we shall express the amount of NiO and Fe in monolayers (ML), always referring to the amount of material deposited (for NiO 1 ML=2.09 Å and for Fe 1 ML =1.43 Å). After the growth *in situ* x-ray photoelectron spectroscopy (XPS) was used to check the film thickness, their stoichiometry and to measure the evolution of the interface chemistry during *in situ* thermal treatments. *In situ* noncontact atomic force microscopy (nc-AFM) and scanning tunneling microscopy (STM) were used to image the NiO and Fe film morphology, respectively. The analysis of the scanning-probe images has been performed by the WSxM[35] program and other commercial software products. The magnetization loops were measured by means of a magneto-optical Kerr effect (MOKE) apparatus, operating either *in situ* or *ex situ*. For *in situ* MOKE measurements the sample was positioned in an aluminum end section of the UHV chamber, in turn placed between the polar expansions of an electromagnet, and the laser light was let in and out of the UHV chamber through nonbirefringent, stress-free glass windows. For *ex situ* MOKE measurements the samples were capped by a 3.5 nm thick Ag layer and a 3 nm thick MgO layer to prevent oxidation during exposure of the samples to atmospheric pressure. The MOKE measurements were performed in the longitudinal configuration with the laser beam impinging at 22.5° from sample normal. The incident beam polarization in some of the measurements was varied form *s* to *p*, *sp*, and *ps* polarizations (i.e., with the electric field perpendicular, parallel, at 45° and at −45° from the incidence plane, respectively). Since for our sample the assumption $|n| \gg 1$, where n is the refraction index of the reflecting medium, is verified, we could obtain the longitudinal, transverse, and polar components of the magnetization M_l, M_t and M_p, by linear combinations of the reflected intensity in *s*, *p*, *sp*, and $-sp$ polarizations, I_s, I_p, I_{sp}, and I_{-sp}, respectively. In particular, we have $I_s + I_p \propto M_l$, $I_s - I_p \propto M_p$, $I_{sp} + I_{-ps} \propto M_p$, and $I_{sp} - I_{-ps} \propto M_t$.[36] The MOKE signal has been normalized to the saturation value of the magnetization for each sample, therefore only relative values of the magnetization are shown.

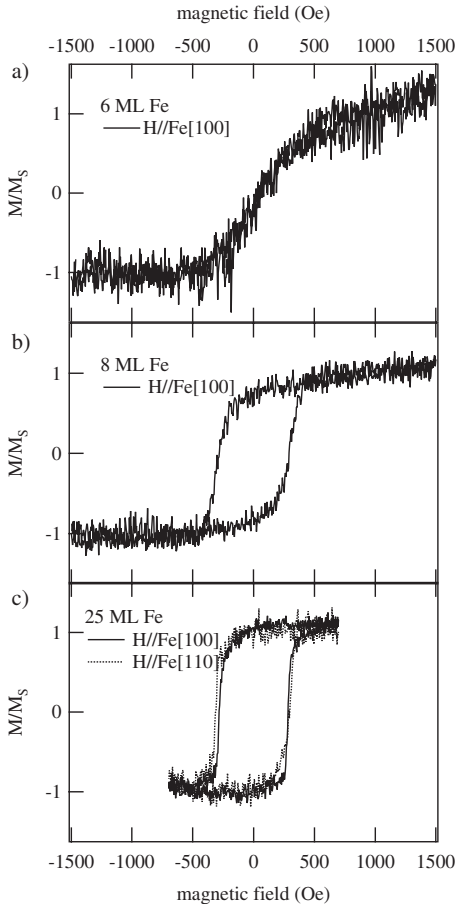

FIG. 1. MOKE longitudinal hysteresis loops for Fe films of different thickness [(a) 6 ML, (b) 8 ML, and (c) 25 ML] on 10 ML NiO/Ag(001) measured with the field along the Fe[100] direction. Panel (c) also reports the hysteresis loop measured with the field along the [110] in plane direction.

In situ thermal treatments were performed by using an electron beam heater, while field cooling (FC) treatments were performed *ex situ* in a low-vacuum (5×10^{-3} Torr) resistive heating furnace. During FC treatments the sample was kept at the desired temperature for 5 min and then slowly (20 K/min) cooled in an external magnetic field of 3000 Oe applied along the Fe [100] direction on the sample surface and perpendicular to the direction of the projection of the Fe growth axis.

III. RESULTS AND DISCUSSION

A. Onset of ferromagnetism

We first investigated the variations of the hysteresis loop as a function of the Fe layer thickness. This investigation was possible due to the availability of MOKE magnetometry operating *in situ*, since the magnetic properties of ultrathin Fe deposits may be influenced by the presence of capping layers. Figure 1 reports the hysteresis loops measured *in situ* in *p* polarization on samples of variable Fe thickness grown

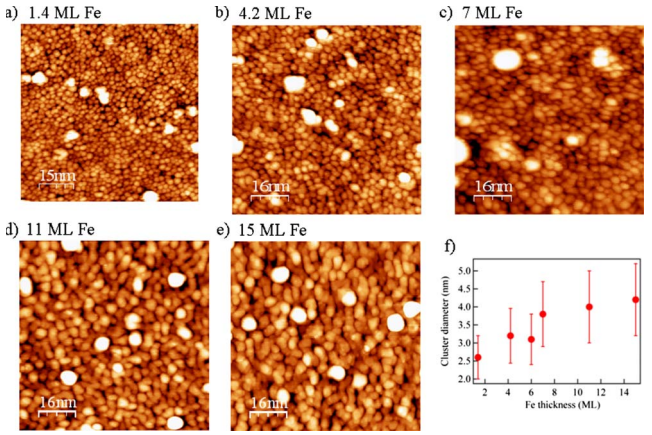

FIG. 2. (Color online) STM images measured for Fe layers of (a) 1.4 ML, (b) 4.2 ML, (c) 7 ML, (d) 11 ML, and (e) 15 ML on 10 ML NiO/Ag(001) (I=0.2 nA, V=1 V). The evolution of the average cluster diameter with Fe thickness is shown in (f), where the error bars are the standard deviation of the size distribution of the clusters measured on 80×80 nm^2 images.

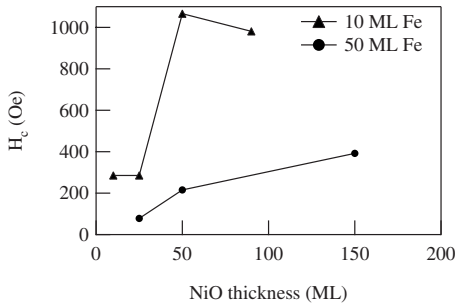

FIG. 3. Coercive fields measured on MOKE longitudinal loops for a 10 ML Fe film and a 50 ML Fe film as a function of NiO thickness.

on a 10 ML NiO film. In systems where a zero or a very small component of the magnetization in the polar direction is expected, MOKE hysteresis cycles in p or s polarization represent the longitudinal magnetization component. The magnetization loops showed no hysteresis at 6 ML and below [Fig. 1(a)]. Above 8 ML the magnetization loops show hysteresis with coercive field of approximately 300 Oe [Fig. 1(b)]. The loop shape does not change significantly for larger Fe thickness and for different in-plane orientation of the applied magnetic field [Fig. 1(c)]. Although the system is epitaxial, magnetocrystalline anisotropy effects on the hysteresis cycles could not be detected as long as the Fe thickness is small enough (below $\sim$50 ML). These are probably masked by the coupling between Fe and NiO, as discussed in Sec. III B.

We rule out the possibility that the absence of hysteresis loop below 6 ML can be due to the formation of non magnetic Fe phases at the interface. Although we know from our previous characterization of the system that the interface is not chemically sharp,[24,25,28] the formation of the FeO-like layer cannot be the only factor responsible for the absence of hysteresis up to 6 ML, since it is extended over no more than 1 or 2 atomic layers.[25] The bct Fe–Ni alloyed phase extends in thickness up to a few atomic layers,[28] but we demonstrated that already a few ML above the interface the magnetic properties are very similar to the ones of pure metallic Fe.[37] Therefore, we considered the possibility for the observed onset of FM behavior to be due to growth morphology. It has to be noted that on a system very similar under the structural point of view, i.e., the Fe/MgO system, the onset of FM behavior has been ascribed to a partial coalescence of the islands at similar coverages.[38] Similarly on the Fe/NiO system we investigated the evolution of the growth morphology with Fe thickness by STM. Figure 2(a) shows an STM image of 1.4 ML Fe deposited on a 10 ML NiO film. At this low coverage Fe forms small clusters with an almost round shape and average lateral size of approximately 2.5 nm. The low-density highest round structures (white in the image) are ascribed to inhomogeneities in the Ag sample surface. With increasing Fe deposition to 4.2 ML [Fig. 2(b)], the islands tend to grow in size. By further increasing the deposition to 7, 11 and 15 ML [Figs. 2(c)–2(e)] not only the cluster size increases [Fig. 2(f)], but the islands also tend to change shape and become more interconnected. This change in morphology is probably responsible for the onset of FM behavior. At low coverage, the particles are too small to have a stable ferromagnetic coupling at RT. By increasing the deposited Fe amount the particles are large enough to have a blocking temperature above RT. A quantitative evaluation of the blocking temperatures by the Néel relaxation formula requires an evaluation of the volumes of the particles (which can be obtained from the STM images) and the determination of their magnetic anisotropy. This last parameter is difficult to be estimated, being largely influenced by the surface contribution, by the shape of the particles, by their mutual interaction and by the coupling with NiO.

B. Magnetization reversal mechanism

The hysteresis loops shown in Figs. 1(b) and 1(c) have a coercivity of a few hundreds Oe, which does not change significantly with Fe thickness up to 25 ML. This value is markedly larger than the one measured on Fe layers with comparable structure, morphology, and thickness grown on MgO/Ag(001) films with very similar procedures,[38] namely, 10–20 Oe. The large values of coercivity are due to coupling with the NiO, and are frequently observed on other FM/AF systems.[33,39,40] We investigated the evolution of the coercivity with NiO thickness for Fe layers of fixed thickness. Figure 3 shows its behavior for a 10 and 50 ML Fe film. In the first case the coercive field increases from about 300 Oe at NiO thickness below 25 ML to values around 1000 Oe for NiO thickness above 50 ML. For the 50 ML Fe film the coercivity values are lower than the corresponding ones for the 10 ML Fe film and they increase with NiO thickness also in this case. We investigated the possibility that this effect can be due to morphological variations: an increased roughness of the thicker NiO films would imply a larger contact area at the interface with Fe and NiO and possibly also a different morphology of the Fe layers, which may cause the observed increase in coercivity. In order to elucidate this

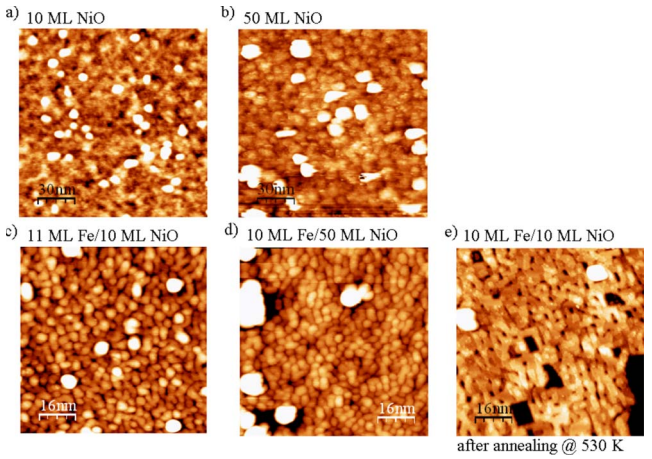

FIG. 4. (Color online) Nc-AFM images of (a) 10 ML and (b) 50 ML NiO films on Ag(001). STM images of (c) 11 ML Fe/10 ML NiO and (d) 10 ML Fe/50 ML NiO as grown and (e) 11 ML Fe/10 ML NiO after annealing at 530 K (I=0.05 nA, V=3 V).

aspect we used nc-AFM to measure the morphology of NiO films of different thickness. Figure 4 a shows the topography of a 10 ML NiO film, where irregular structures not uniform in size are present. The average surface roughness is below 2 atomic layers. We did not observe any morphological anisotropy in spite of the oblique incidence growth of the NiO films, in analogy with previous works.[33] A few highest round structures (white in the image), approximately 5 nm large and 2–2.5 nm high, are ascribed, as already mentioned, to inhomogeneities in the Ag sample surface, acting as nucleation centers for NiO growth. The surface topography of the 50 ML NiO film [Fig. 4(b)] and the 10 ML film are comparable in terms of roughness and irregularity of the structures. Figure 4(c) and 4(d) report the morphology of a Fe film of similar thickness, 11 and 10 ML, grown on the 10 and 50 ML thick NiO films, respectively. As expected, the Fe morphology is not significantly affected by the thickness of the NiO film underneath. In both cases interconnected islands of round shape with average lateral size of 3–4 nm and height of 1–2 nm can be observed. Having excluded morphology dependent effects, in order to explain the coercivity of our system and, more in general, magnetization reversal, we have to investigate the intrinsic magnetic couplings that come into play. In the literature different models have been proposed to explain the coercivity of FM/AF systems. In general, two different mechanisms are invoked: instabilities in the antiferromagnet[41,42] and/or inhomogeneous magnetization reversal.[42–44] The first mechanism occurs close to the blocking temperature of the system because the AF material reverses its spins due to the coupling with the FM material and its contribution increases with increasing weight of the interface coupling and decreases with increasing AF anisotropy. The second mechanism is due to irreversible processes in the ferromagnetic layer, occurring due to the presence of antiferromagnetic grains with different orientations. Both effects may come into play in our system, and both may have an increasing weight with increasing AF layer thickness, due to an increase in its magnetic anisotropy.

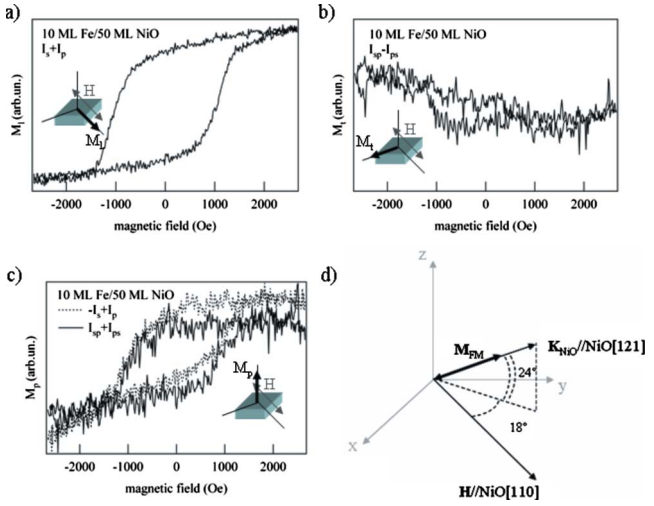

FIG. 5. (Color online) Linear combinations of MOKE longitudinal hysteresis loops in different polarizations, giving the (a) longitudinal, (b) transverse, and (c) polar components of the magnetization for a 10 ML Fe film on 50 ML NiO. (d) Main anisotropy directions for the system and schematic view of the mechanism for magnetization reversal.

In order to have a complete picture of magnetization reversal for our system, we measured the MOKE hysteresis cycles in *s*, *p*, *sp*, and *ps* polarizations and obtained the longitudinal (M_l), transverse (M_t), and polar (M_p) components of the magnetization by linear combinations of the three spectra (see Sec. II). For each graphic shown in Figs. 5 and 6 the magnetization is reported in arbitrary units because the experimental setup does not allow to reach the saturation magnetization in the polar and transverse directions. In Figs. 5 and 6, we show the behavior of M_l, M_t, and M_p for the most significant samples, i.e., a 10 ML Fe/50 ML NiO bi-

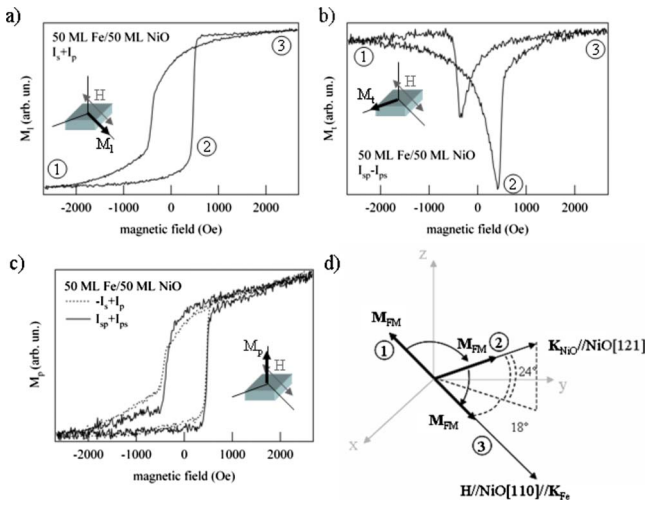

FIG. 6. (Color online) Linear combinations of MOKE longitudinal hysteresis loops in different polarizations, giving the (a) longitudinal, (b) transverse, and (c) polar components of the magnetization for a 50 ML Fe film on 50 ML NiO. (d) Main anisotropy directions for the system and schematic view of the mechanism for magnetization reversal.

layer, in which the FM layer thickness is much smaller than the AF one, and a 50 ML Fe/50 ML NiO layer, in which the FM and AF layer thickness are comparable. On the 10 ML Fe/50 ML NiO bilayer, the longitudinal component of the magnetization [Fig. 5(a)] shows a loop, but the magnetization is not completely saturated even at the largest fields used. A cycle, though with a lower signal-to-noise ratio than the one of the longitudinal component, is observed for the polar component of the magnetization [Fig. 5(c)]. The transverse component instead shows a residual cycle, which is hardly distinguishable within the noise level [Fig. 5(b)]. As shown in Fig. 5(d), the NiO[121] direction, which is the anisotropy direction for NiO closest to the direction of the applied field (H∥Fe[100]∥NiO[110]), forms an angle of 24° with the *xy* plane and its projection in the *xy* plane forms an angle of 18° with the H direction. The behavior of the three magnetization components is interpreted assuming that the magnetization reversal of the 10 ML Fe/50 ML NiO film proceeds by nucleation of reversed domains and domain wall motion. Most of the film has an in plane magnetization which reverses in the direction of the applied field. A small part of the domains however seem to reverse their magnetization along the anisotropy direction of NiO closest to the external field direction.[33] These domains would have a component along the polar direction and a smaller component along the transverse direction, even at the largest fields used in this study. The fact that the MOKE cross section is much larger for the polar magnetization component than for the transverse one[45] can explain the very low signal in the transverse direction. For these domains the interface coupling dominates over the coupling with the rest of Fe layer and with the external magnetic field. We expect this phase to be confined at the Fe/NiO interface, where an epitaxial intermixed phase is present.[22–25] The high value of coercive field measured at low Fe coverages originates from this phase.

The situation for a 50 ML Fe/50 ML NiO bilayer is markedly different, as can be seen in Fig. 6. The longitudinal component of the magnetization [Fig. 6(a)] shows a loop with an asymmetry between the ascending and descending branches. Along the ascending branch the magnetization switches direction within a relatively small field range. The descending branch instead shows a more gradual inversion of the magnetization. The transverse loop [Fig. 6(b)] shows two peaks at values corresponding to the inversion fields along the two branches. This indicates that part of the magnetization rotates in the plane during reversal. The polar component shows an open loop [Fig. 6(c)]. Asymmetric loop shapes have often been observed in systems where an uniaxial anisotropy and a unidirectional anisotropy not perfectly aligned[39,40,46–48] cause a different reversal mechanism along the two branches of the hysteresis loop. In our system the anisotropy along the NiO[121] direction may be larger than the other NiO anisotropy directions, due to the limited film thickness, favoring the occupation of the domains with a major spin component in plane,[15–17] and to the eventual growth anisotropy.[33] Furthermore, as the Fe thickness is increased to 50 ML a growth anisotropy in the direction perpendicular to Fe growth starts to appear. This is reflected in the steps of the hysteresis loop of Fig. 7, frequently observed in ferromagnetic films deposited at oblique incidence.[49] This

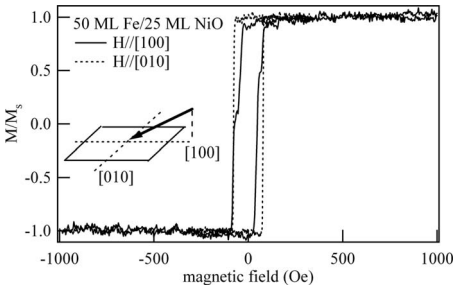

FIG. 7. MOKE longitudinal hysteresis loops of a 50 ML Fe/25 ML NiO bilayer, measured with the field parallel and perpendicular to the projection of the growth direction on the sample plane. A sketch of the growth geometry is also shown in the inset.

anisotropy is typically dependent both on the Fe thickness and on the orientation of the growth axis,[50] in our case 45° from sample normal along the Fe[100]. The magnetization loops in the three directions for a 50 ML film on 50 ML NiO indicate that magnetization reversal proceeds by a mechanism which is neither a coherent in-plane rotation, in which case we would not observe an open loop in the polar component of the magnetization, nor pure formation of reversed domains and domain wall motion, due to the shape of the transverse component of the magnetization. The mechanism for magnetization reversal is different along the ascending and descending branches. Along the ascending branch at fields close to the inversion field of the longitudinal loop some of the domains rotate toward the [121] direction; for increasing fields a decrease in transverse magnetization is observed, indicating a further rotation of most of the domains toward the field direction [Fig. 6(d)]. The polar magnetization loop indicates that also on this sample a phase, probably situated at the interface, remains bound to the [121] direction and presents a polar net magnetization. For decreasing fields, the unidirectionality of the anisotropy along the [121] direction makes the reversal process more gradual, although the same two mechanisms (rotation and domain wall propagation) come into play. The unidirectionality of the NiO anisotropy direction may come from morphological effects, since no FC procedure was applied to these samples. The increasing weight of the noninterfacial Fe phase with increasing Fe thickness is probably responsible for the decrease in coercive field at large Fe thickness (Fig. 3).

The shape of the hysteresis loops is the same after repeated cycling, indicating that there are no irreversible effects in the AF material.

C. Thermal stability

Before performing FC of the samples, we checked the thermal stability of the interface by XPS, using an 8 ML thick Fe sample, in order to have a good compromise between the signal-to-noise ratio and the sensitivity to the interface layers. The Ni 2*p* and Fe 2*p* XPS spectra for different values of heating temperatures are shown in Fig. 8. Already at 290 K the Ni 2*p* spectra show a Ni^{2+} component and a metallic component, in agreement with previous works,[23,24,28] corresponding to a reduction of ~0.8 ML NiO

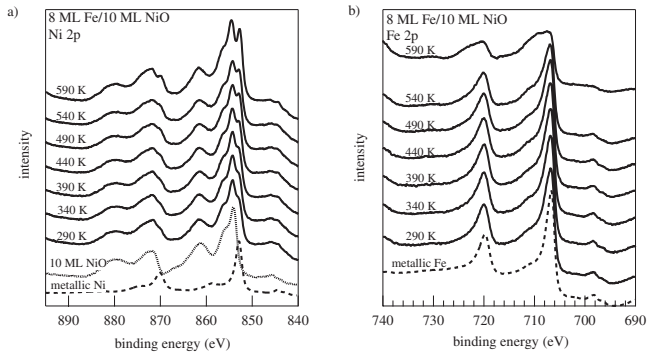

FIG. 8. Evolution of (a) Ni $2p$ and (b) Fe $2p$ XPS lineshapes of an 8 ML Fe/10 ML NiO bilayer with progressive annealing temperatures from RT to 590 K. Reference spectra of a 10 ML NiO film and of a metallic Ni sample are also shown in the bottom part of panel (a). A reference spectrum of a metallic Fe sample is also reported in the bottom part of panel (b).

and an oxidation of ~0.8 ML Fe. In the Fe $2p$ spectra at 290 K the intensity ratio between the $2p_{3/2}$ peak at 707 eV and the broad shoulder at ~710 eV binding energy is slightly larger than on a bulk Fe film. No significant changes in the XPS spectra are observed after *in situ* heating the samples up to 440 K. At 490 K, a slight increase in the Ni^0 to Ni^{2+} component is observed, corresponding to a reduction of 1 ML NiO, while at 590 K the Ni reduction and Fe oxidation are relevantly increased. The morphology of a 10 ML Fe/10 ML NiO bilayer after heating at 530 K is shown in Fig. 4(e). The Fe islands are much more interconnected, forming a network of structures with edges parallel to the Fe[100] direction and holes with an almost rectangular shape.

D. Exchange bias

After checking that the samples are chemically stable at least up to temperatures of 490 K, we measured the hysteresis loops after FC for different values of the Fe and NiO layer thickness. The results are summarized in Fig. 9. For NiO films below 25 ML no exchange bias can be observed, whatever the Fe layer thickness is. This is shown in Fig. 9(a), in the case of a 12 ML Fe/10 ML NiO bilayer after FC to 490 K. No significant change of the hysteresis loop can be observed for such bilayers after FC up to temperatures of 540 K (spectrum not shown). This indicates that the morphological changes after annealing [see Fig. 4(e)] do not imply significant changes in the magnetic couplings. The Fe grains are already interconnected and a smoothing of their surface and of their grain boundaries does not have significant consequences on magnetization reversal. With increasing NiO thickness to 50 ML, together with the already discussed increase in coercivity of the loops, a negative EB (i.e., in the direction opposite to the applied field) of a few hundreds Oe is present after FC [Fig. 9(b)]. No significant variation in coercivity after FC is observed. The EB field does not change significantly with increasing FC temperatures up to 540 K. The existence of a critical AF layer thickness for the onset of EB is a well known phenomenon[51] which has been ascribed to two possible mechanisms. The first is a decrease

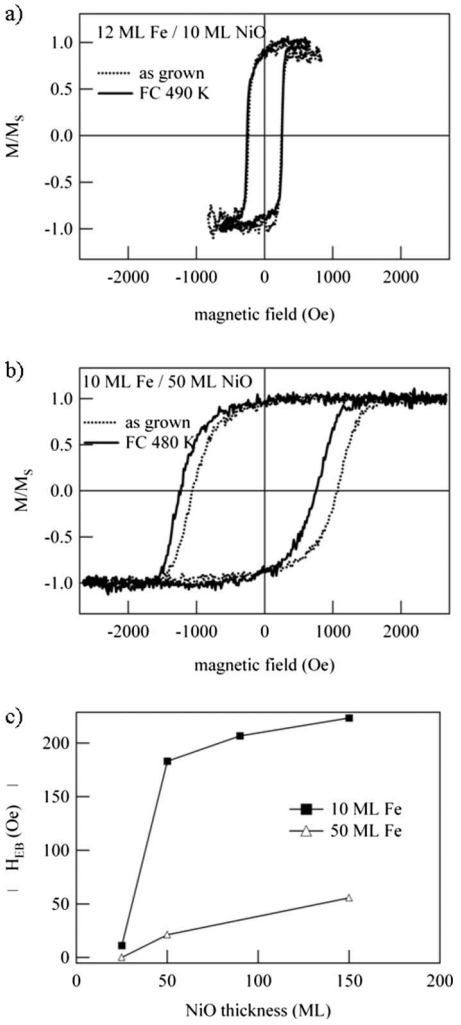

FIG. 9. MOKE longitudinal hysteresis cycles for (a) a 10 ML Fe/10 ML NiO sample and (b) a 10 ML Fe/50 ML NiO sample as grown and after FC. (c) Dependence of the EB field on the NiO thickness for 10 and 50 ML Fe films.

in T_N with AF layer thickness, which for a certain thickness becomes lower than the measuring temperature and prevents the occurrence of EB. For our system, since we know that the T_N of NiO/Ag layers is above RT already for thickness of 6 ML,[17] we exclude the possibility that this effect can play a role. A second point that has to be considered is the fact that the anisotropy energy of the AF material has to be larger than the interface coupling energy for EB to be observed. This is probably the effect which comes into play for our system. The increase in anisotropy of the NiO film with thickness is the origin of the increase in coercive field and of exchange bias field with NiO thickness. At 10 ML the NiO film anisotropy is large enough to give relatively large coercivities through coupling with the Fe overlayer, but not enough to pin it after FC. The measured critical NiO thickness for the onset of EB in our samples is between 25 and 50 ML and the EB and coercive fields continue to increase at 150 ML [Figs. 3 and 9(c)], indicating that probably the anisotropy has not reached its saturation value for such a thickness. The large

NiO thickness range over which the EB increases is due to the relatively low value of anisotropy of bulk NiO compared to other AF materials. As expected, the EB field inversely depends on the Fe layer thickness, approximately as $1/t_{Fe}$, indicating that exchange bias is an interfacial effect. The maximum values for EB are obtained for 10 ML Fe films, to be largely above the onset for ferromagnetism, on the thickest NiO films used for this study, i.e., 150 ML. The maximum EB field obtained is 220 Oe, largely higher than the values obtained for polycrystalline Fe/NiO systems,[33,34] or for other FM layers on NiO.[52]

The decrease in exchange bias field for Fe layers of larger thickness (Fig. 9(c)) can be correlated with the formation of a second magnetic phase at larger Fe thickness, discussed in Sec. III B. This phase is relatively less strongly coupled to the NiO underlayer than the interface phase and its weight increases with thickness, thus reducing the net exchange bias field.

We did not observe a significant training effect, i.e., a decrease in EB for repeated cycling, not even after several tens of cycles. The absence of training effect indicates that the irreversible processes in the AF layer, frequently observed in polycrystalline samples[53] or in systems grown in less controlled conditions,[54] do not occur in epitaxial NiO layers.

IV. CONCLUSIONS

We have investigated the magnetic properties of epitaxial Fe films on NiO(001) layers. We found that ultrathin (i.e., below 6 ML) Fe layers do not show a ferromagnetic behavior, because they are discontinuous. Fe films with intermediate thickness (around 10 ML) show hysteresis cycles with large coercivity, due to a strong coupling with the underlying NiO. The magnetization reversal proceeds via nucleation of inverse domains and domain wall motion, with a significant part of the magnetization pinned to the AF layer anisotropy direction. For thicker Fe layers, the interplay between unidirectional growth anisotropy and the uniaxial anisotropy of NiO induces an asymmetric magnetization reversal with the interfacial layers pinned to NiO and the upper layers partially rotating in the sample plane. Exchange bias on this system can be established only if the NiO layer thickness is above 25 ML, probably because the anisotropy of thinner films is not strong enough to produce the required pinning. Values of EB field as high as 220 Oe can be obtained by properly choosing the Fe and NiO layer thickness. No training effect has been measured on this system. This work shows that a detailed characterization of FM/AF systems can be of great help to unravel the complicated microscopic couplings that determine their magnetic behavior.

[1] S. Yuasa, T. Nagahama, A. Fukushima, and Y. Suzuki, Nature Mater. **3**, 868 (2004).
[2] H. Ohldag, T. J. Regan, J. Stöhr, A. Scholl, F. Nolting, J. Lüning, C. Stamm, S. Anders, and R. L. White, Phys. Rev. Lett. **87**, 247201 (2001).
[3] W. Kuch, L. I. Chelaru, F. Offi, J. Wang, M. Kotsugi, and J. Kirschner, Nature Mater. **5**, 128 (2006).
[4] M. Finazzi, L. Duò, and F. Ciccacci, Surf. Sci. Rep. **62**, 337 (2007).
[5] R. Abrudan, J. Miguel, M. Bernien, C. Tieg, M. Piantek, J. Kirschner, and W. Kuch, Phys. Rev. B **77**, 014411 (2008).
[6] H. Ohldag, A. Scholl, F. Nolting, E. Arenholz, S. Maat, A. T. Young, M. Carey, and J. Stöhr, Phys. Rev. Lett. **91**, 017203 (2003).
[7] W. H. Meiklejohn and C. P. Bean, Phys. Rev. **102**, 1413 (1956); **105**, 904 (1957).
[8] J. Nogués and I. K. Schuller, J. Magn. Magn. Mater. **192**, 203 (1999).
[9] A. E. Berkowitz and K. Takano, J. Magn. Magn. Mater. **200**, 552 (1999).
[10] D. Mauri, H. C. Siegmann, P. S. Bagus, and E. Kay, J. Appl. Phys. **62**, 3047 (1987).
[11] A. P. Malozemoff, Phys. Rev. B **35**, 3679 (1987).
[12] A. P. Malozemoff, J. Appl. Phys. **63**, 3874 (1988).
[13] A. P. Malozemoff, Phys. Rev. B **37**, 7673 (1988).
[14] N. C. Koon, Phys. Rev. Lett. **78**, 4865 (1997).
[15] D. Alders, L. H. Tjeng, F. C. Voogt, T. Hibma, G. A. Sawatzky, C. T. Chen, J. Vogel, M. Sacchi, and S. Iacobucci, Phys. Rev. B **57**, 11623 (1998).
[16] S. Altieri, M. Finazzi, H. H. Hsieh, H.-J. Lin, C. T. Chen, T. Hibma, S. Valeri, and G. A. Sawatzky, Phys. Rev. Lett. **91**, 137201 (2003).
[17] S. R. Krishnakumar, M. Liberati, C. Grazioli, M. Veronese, S. Turchini, P. Luches, S. Valeri, and C. Carbone, J. Magn. Magn. Mater. **310**, 8 (2007).
[18] S. D. Peacor and T. Hibma, Surf. Sci. **301**, 11 (1994).
[19] K. Marre, H. Neddermeyer, A. Chassé, and P. Rennert, Surf. Sci. **357-358**, 233 (1996).
[20] M. Portalupi, L. Duò, G. Isella, R. Bertacco, M. Marcon, and F. Ciccacci, Phys. Rev. B **64**, 165402 (2001).
[21] E. Groppo, C. Prestipino, C. Lamberti, R. Carboni, F. Boscherini, P. Luches, S. Valeri, and S. D'Addato, Phys. Rev. B **70**, 165408 (2004).
[22] T. J. Regan, H. Ohldag, C. Stamm, F. Nolting, J. Lüning, J. Stöhr, and R. L. White, Phys. Rev. B **64**, 214422 (2001).
[23] R. de Masi, D. Reinicke, F. Müller, P. Steiner, and S. Hüfner, Surf. Sci. **515**, 523 (2002).
[24] P. Luches, M. Liberati, and S. Valeri, Surf. Sci. **532-535**, 409 (2003).
[25] P. Luches, V. Bellini, S. Colonna, L. Di Giustino, F. Manghi, S. Valeri, and F. Boscherini, Phys. Rev. Lett. **96**, 106106 (2006).
[26] C. Tusche, H. L. Meyerheim, F. U. Hillebrecht, and J. Kirschner, Phys. Rev. B **73**, 125401 (2006).
[27] L. Duò, M. Portalupi, M. Marcon, R. Bertacco, and F. Ciccacci, Surf. Sci. **518**, 234 (2002).
[28] S. Benedetti, P. Luches, M. Liberati, and S. Valeri, Surf. Sci. **572**, L348 (2004).
[29] H. Matsuyama, C. Haginoya, and K. Koike, Phys. Rev. Lett. **85**,

646 (2000).
[30] W. Zhu, L. Seve, R. Sears, B. Sinkovic, and S. S. P. Parkin, Phys. Rev. Lett. **86**, 5389 (2001).
[31] H. Ohldag, A. Scholl, F. Nolting, S. Anders, F. U. Hillebrecht, and J. Stohr, Phys. Rev. Lett. **86**, 2878 (2001).
[32] M. Finazzi, Phys. Rev. B **69**, 064405 (2004).
[33] M. Cartier, S. Auffret, Y. Samson, P. Bayle-Guillemaud, and B. Dieny, J. Magn. Magn. Mater. **223**, 63 (2001).
[34] L. Fan, S. Gang, J. Dogmei, S. Wangzhou, and M. Xueming, J. Alloys Compd. **427**, 50 (2007).
[35] I. Horcas, R. Fernández, J. M. Gómez-Rodríguez, J. Colchero, J. Gómez-Herrero, and A. M. Baro, Rev. Sci. Instrum. **78**, 013705 (2007).
[36] P. Vavassori, Appl. Phys. Lett. **77**, 1605 (2000).
[37] P. Luches, S. Benedetti, L. Pasquini, F. Boscherini, M. Zajac, J. Korecki, R. Rüffer, and S. Valeri, Nucl. Inst. Met. B **268**, 361 (2010).
[38] P. Torelli, S. Benedetti, P. Luches, L. Gragnaniello, J. Fujii, and S. Valeri, Phys. Rev. B **79**, 035408 (2009).
[39] M. R. Fitzsimmons, P. Yashar, C. Leighton, I. K. Schuller, J. Nogués, C. F. Majkrzak, and J. A. Dura, Phys. Rev. Lett. **84**, 3986 (2000).
[40] F. Radu, M. Etzkorn, R. Siebrecht, T. Schmitte, K. Westerholt, and H. Zabel, Phys. Rev. B **67**, 134409 (2003).
[41] E. Fulcomer and S. H. Charap, J. Appl. Phys. **43**, 4190 (1972).
[42] M. D. Stiles and R. D. McMichael, Phys. Rev. B **63**, 064405 (2001).
[43] S. Zhang, D. V. Dimitrov, G. C. Hadjipanayis, J. W. Cai, and C. L. Chien, J. Magn. Magn. Mater. **198-199**, 468 (1999).
[44] Z. Li and S. Zhang, Phys. Rev. B **61**, R14897 (2000).
[45] Z. J. Yang and M. R. Scheinfein, J. Appl. Phys. **74**, 6810 (1993).
[46] J. McCord, R. Schäfer, R. Mattheis, K.-U. Barholz, J. Appl. Phys. **93**, 5491 (2003).
[47] B. Beckmann, U. Nowak, and K. D. Usadel, Phys. Rev. Lett. **91**, 187201 (2003).
[48] J. Camarero, J. Sort, A. Hoffmann, J. M. García-Martín, B. Dieny, R. Miranda, and J. Nogués, Phys. Rev. Lett. **95**, 057204 (2005).
[49] Y. Park, E. E. Fullerton, and S. D. Bader, Appl. Phys. Lett. **66**, 2140 (1995).
[50] Q. Zhan, C. Van Haesendonck, S. Vandezande, and K. Temst, Appl. Phys. Lett. **94**, 042504 (2009).
[51] M. S. Lund, W. A. A. Macedo, K. Liu, J. Nogués, I. K. Schuller, and C. Leighton, Phys. Rev. B **66**, 054422 (2002).
[52] Z. Qian, J. M. Sivertsen, and J. H. Judy, J. Appl. Phys. **83**, 6825 (1998).
[53] S. G. E. te Velthuis, A. Berger, G. P. Felcher, B. K. Hill, and E. Dan Dahlberg, J. Appl. Phys. **87**, 5046 (2000).
[54] A. Hochstrat, Ch. Binek, and W. Kleemann, Phys. Rev. B **66**, 092409 (2002).